

STRIPLINE BEAM IMPEDANCE*

A. Blednykh[#], W. Cheng, S. Krinsky
 BNL, Photon Science, NY 19973-5000, USA

Abstract

We discuss the Lambertson and Shafer formalisms for the longitudinal and transverse beam impedances of a stripline. The required characteristic impedances and the geometric factors are determined by the solution of Laplace's equation in 2-dimensions, which we find using the 2-D POISSON code. Lambertson's equations are compared with numerical results obtained using the 3-D electromagnetic simulation code GdfidL. Good agreement is found at low frequencies. The results differ at high frequencies, since the analytic results do not take into account higher order modes.

INTRODUCTION

Striplines [1-4] are often used in accelerator systems to serve as either pick-ups or kickers. These devices are comprised of the conducting surfaces of the vacuum envelope and inner conducting electrodes as illustrated in Fig. 1. An important issue in the design of a stripline is the impedance that it presents to the particle beam traveling along the axis through the device.

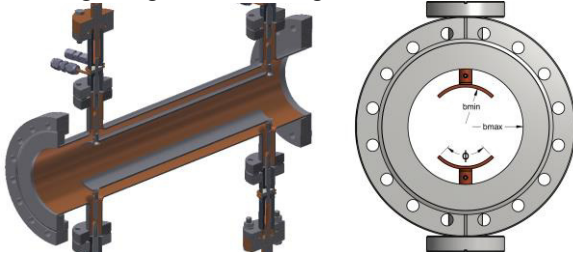


Figure 1: One half of the stripline kicker geometry. Two electrodes are located inside of the round pipe with $b_{min} = 24.1mm$ and $b_{max} = 38mm$ radii. The length of electrodes is 300mm. The electrode thickness is 2mm.

Lambertson [2,3] has presented a very interesting and comprehensive discussion of pick-ups and kickers. Following his formalism, one can express the longitudinal and transverse (vertical) beam impedances for a stripline in the form

$$Z_{||}(k) = g_{||}^2 Z_{ch,||} [\sin^2(kL) + j \sin(kL) \cos(kL)] \quad (1)$$

$Z_{\perp}(k) = (g_{\perp}^2 Z_{ch,\perp} / kb^2) [\sin^2(kL) + j \sin(kL) \cos(kL)] \quad (2)$
 where k is the wave number, L is the longitudinal length of electrodes, b_{min} is the minimum distance between the beam axis and the electrodes, $g_{||}$ and g_{\perp} are longitudinal and transverse geometric factors, and $Z_{ch,||}$ and $Z_{ch,\perp}$ are longitudinal and transverse characteristic impedances of the stripline. The geometric factors and the characteristic impedances are for the full structure containing all electrodes. We note that for a device comprised of two identical electrodes symmetrically placed as in Fig. 1,

$Z_{ch,||} = Z_L/2$, where Z_L is the characteristic impedance of a single electrode.

At low frequency the longitudinal shunt impedance is related to the longitudinal beam impedance by [3]

$$R_{sh,||} = Re Z_{||}(k) \times 4, \quad (3)$$

and the transverse shunt impedance is related to the transverse beam impedance by

$$R_{sh,\perp} = Re Z_{\perp}(k) \times 4/k \quad (4)$$

To determine $Z_{ch,||}$ and $Z_{ch,\perp}$ for a given geometry, one needs to solve Laplace's equation in 2 dimensions. For this, we use the 2D POISSON electrostatic code [5]. The characteristic impedance is given by [6]

$$Z_{ch} = \frac{1}{cC}, \quad (5)$$

where c is the velocity of light and C is the capacitance of the stripline structure. For the longitudinal mode, both electrodes have voltage V_p , while for the transverse mode they have voltages of opposite polarity $\pm V_p$. In both cases, the capacitance is related to the stored energy W_e and voltage V_p via

$$C = \frac{2W_e}{V_p^2} \quad (6)$$

Given the magnitude of the voltage V_p , we calculate the stored energy using POISSON and in this manner determine the capacitance and thus the characteristic impedance for each mode.

First, as an illustration, we consider the ideal coaxial transmission line with geometric parameters $b_{min} = 24.1mm$ inner and $b_{max} = 38mm$ outer radius (Fig. 2a). The characteristic impedance determined from the stored energy computed by POISSON and using Eqs. (5 and 6) with specified positive voltage ($V_p = +1Volt$) on inner conductor is $Z_{ch}^+ = 22.53\Omega$. This agrees with the well-known result, $Z_{ch}^{CXL} = \frac{Z_0}{2\pi} \text{Log}(b_{max}/b_{min})$ for the coaxial (CXL) transmission line.

Next, we consider the longitudinal and transverse characteristic impedances for the round stripline geometry shown in Fig. 2b,c. The electrode radius b_{min} and outer radius b_{max} are fixed. The angle subtended by an electrode is varied from $\phi = 10^\circ$ to $\phi = 170^\circ$. The longitudinal and transverse characteristic impedances of the structure with the two electrodes as a function of the electrode angle are shown in Fig. 3. The longitudinal characteristic impedance tends to 23Ω for $\phi \rightarrow 180^\circ$, approaching the result for the coaxial transmission line, as it must.

As can be seen from Fig. 3, for electrode angle $\phi \rightarrow 180^\circ$, the transverse characteristic impedance $Z_{ch,\perp}$ is about a factor of two less than the longitudinal $Z_{ch,||}$. For electrode angle $\phi \rightarrow 90^\circ$, their difference becomes

*Work supported by DOE contract DE-AC02-98CH10886.

[#]blednykh@bnl.gov

less but the fact that they are not equal means that a pair of electrodes matched to 25Ω transversally (50Ω single electrode) are mismatched longitudinally ($Z_{ch,\parallel} = 18.2\Omega$) and vice versa.

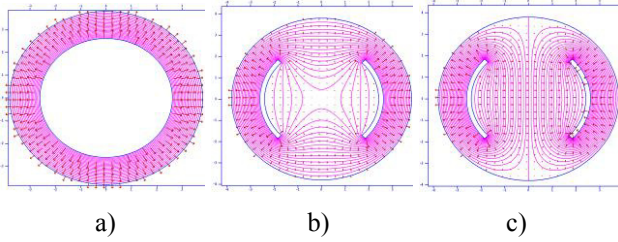


Figure 2: a) Coaxial transmission line with inner and outer radii of $b_{min} = 24.1mm$ and $b_{max} = 38mm$ respectively. b) Longitudinal excitation for $\phi = \pi/2$: two electrodes inside the round pipe at equal positive voltages V_p . c) Transverse excitation for $\phi = \pi/2$: two electrodes inside the round pipe at $\pm V_p$. Magenta lines are lines of constant scalar potential. Arrows are proportional to electric field strength.

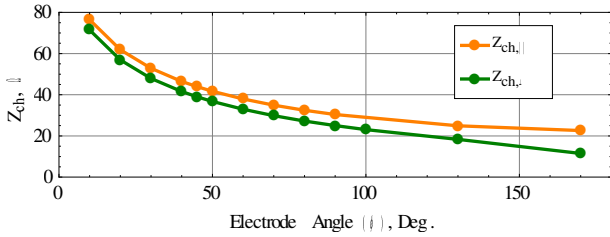


Figure 3: For the structure of Fig. 2b,c, we plot the longitudinal (orange) and transverse (green) characteristic impedances as a function of electrode angle ϕ calculated using the POISSON code.

The geometric factors for a pair of electrodes as a function of the electrode angle ϕ are shown in Fig. 4 (other geometric dimensions fixed). For $\phi \rightarrow \pi$, the longitudinal geometric factor $g_{\parallel} \rightarrow 1$, while the transverse geometric factor, $g_{\perp} \rightarrow 4/\pi$.

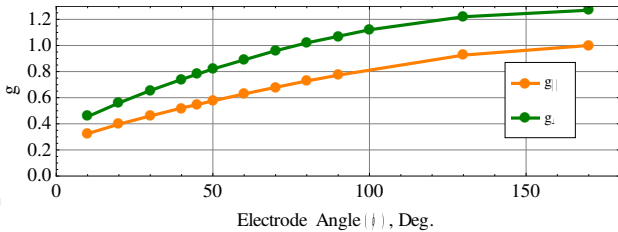


Figure 4: For the structure of Fig. 2b,c, we plot the longitudinal (orange) and transverse (green) geometric factors as a function of electrode angle ϕ calculated using the POISSON code.

BEAM IMPEDANCES, $Z_{\parallel}(k)$ AND $Z_{\perp}(k)$

The real and imaginary parts of the longitudinal beam impedance at low frequencies are shown in Eq. (1) [1].

In Figs. 5a and 5b, we compare Eq. (1) with calculated data obtained using the 3D GdfidL electromagnetic simulation code [7] for the stripline geometry with 90° electrode angle, as shown in Fig. 1. The simulated

longitudinal geometric factor and longitudinal characteristic impedance are $g_{\parallel} = 0.774$ and $Z_{ch,\parallel} = \frac{Z_L}{2} = 30.5\Omega$ (for two electrodes).

We varied the geometric dimensions of the coaxial feed-thru connectors to obtain three different longitudinal characteristic impedances of the external coaxial line, $Z_{ch}^{CXL} = 51\Omega, 61\Omega$ and 100Ω . This was done in order to check the deviation of the GdfidL calculated longitudinal beam impedance from Eq. (1), when electrodes are matched or mismatched to Z_{ch}^{CXL} of the feed-thru connectors.

First, we consider the characteristic impedance of feed-thru connectors $Z_{ch}^{CXL} = 51\Omega$. In this case, there is a good match to the transverse characteristic impedance ($Z_{ch,\perp}$) of each stripline electrode with 90° angle and a mismatch to the longitudinal characteristic impedance ($Z_L = 2Z_{ch,\parallel} = 61\Omega$) of single electrode for the same angle. From Figs. 5a and 5b, we see that the longitudinal beam impedance (real and imaginary parts) agree well with Eq. (1) at low frequencies. The longitudinal impedance spectrum starts to deviate at high frequencies from the shape expected from Eqs. (1,2).

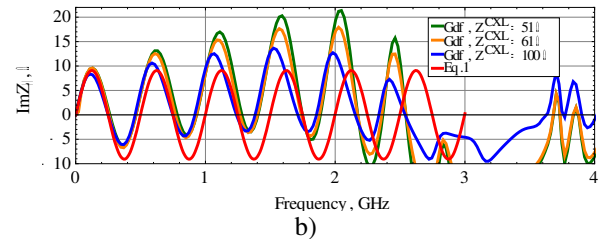
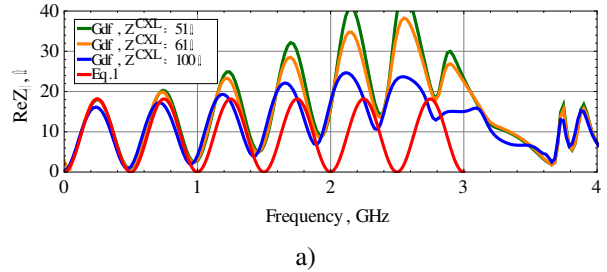


Figure 5: Real (a) and Imaginary (b) part of the longitudinal impedance for the stripline kicker with two 90° angle electrodes inside. The feed-thru connectors are matched to three different characteristic impedances $Z_{ch}^{CXL} = 51\Omega$ (green curve), $Z_{ch}^{CXL} = 61\Omega$ (orange curve) and $Z_{ch}^{CXL} = 100\Omega$ (blue curve). The longitudinal characteristic impedance of two 90° angle electrodes is $Z_{ch,\parallel} = 30.5\Omega$. The red curves are the results of Eq. (1), with $Z_{ch,\parallel} = 30.5\Omega$ and $g_{\parallel} = 0.774$.

Next, we consider the characteristic impedance of feed-thru connectors to be $Z_{ch}^{CXL} = 61\Omega$. In this case the feed-thru connectors are matched to the longitudinal characteristic impedance of each individual electrode. The difference between the numerical results (orange curves in Figs. 5a and 5b) and the analytic results [Eqs. (1)] is reduced at high frequencies (below 3GHz) since matching is improved, but still there is significant

deviation. This can be explained due to gradual increase of the reflection coefficient (S_{11} -parameter) at higher frequencies. The coaxial feedthru connectors and electrode pair are perfectly matched at low frequencies. The reflection of the TEM-mode in the coaxial waveguide is around 10% for considered geometry at low frequencies and 50% at frequency ~ 2 GHz (determined from a GdfidL calculation). Due to larger reflection of TEM-mode from output feed-thru connectors at high frequencies, electromagnetic fields radiate more into the vacuum chamber and the real part of the longitudinal coupling impedance $ReZ_{||}(k)$ deviates from quadratic sinusoidal wave. If the longitudinal characteristic impedance is over-matched ($Z_{ch}^{CXL} = 100\Omega$), then we observe frequency shift and reduction of $Z_{||}(k)$ at low frequencies.

The discussed equations provide a good approximate description of the beam impedance. We found excellent agreement between equation Eq. (1) and numerical calculations at low frequencies, when the electrodes and feed-thru connectors are matched or even slightly mismatched to each other

The real and imaginary parts of the transverse beam impedance are shown in Eq. (2). This equation is compared with GdfidL results for the stripline geometry as shown in Fig. 1. We analysed the effects of two electrodes with an angle of 90° each. The calculated transverse geometric factor and transverse characteristic impedance are $g_{\perp} = 1.1$ and $Z_{ch,\perp} = 25\Omega$ (for two electrodes). The transverse beam impedance is calculated for two different characteristic impedances of the feed-thru coaxial connectors, $Z_{ch}^{CXL} = 51\Omega$ and $Z_{ch}^{CXL} = 61\Omega$ (Fig. 6a and Fig. 6b).

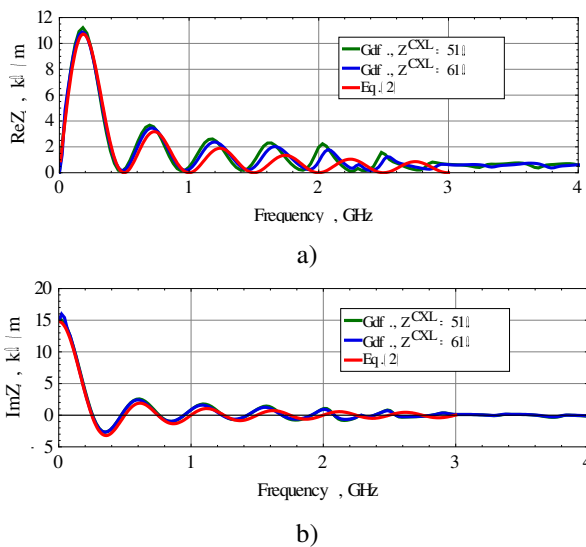


Figure 6: Real (a) and Imaginary (b) part of the transverse impedance of the stripline kicker with two 90° angle electrodes inside. The feed-thru connector has two different characteristic impedances, $Z_{ch}^{CXL} = 51\Omega$ (green) and $Z_{ch}^{CXL} = 61\Omega$ (blue). The red curves are the result of Eq. (2).

As a result the electrodes are well matched in first case and slightly mismatched in the second. The real and imaginary parts of the transverse beam impedance agree well with Eq. (2) up to 2GHz. The imaginary part of the beam impedance at $\omega \rightarrow 0$ is $ImZ_{\perp} = 15k\Omega/m$. The small mismatch of electrodes with connectors has small effect on the transverse beam impedance.

TRANSVERSE SHUNT IMPEDANCE

The transverse shunt impedance has been calculated via Eq. (4). The real part of the transverse beam impedance of Eq. (2) with simulated transverse geometric factor and the transverse characteristic impedance has been implemented into Eq. (4) (green) and the result is shown at low frequency in Fig. 7. It agrees with $R_{sh,\perp}$ data obtained due to implementing the GdfidL data $ReZ_{\perp}(k)$ from Fig. 6a in to Eq. (4).

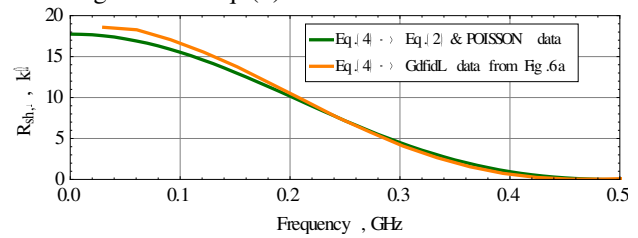


Figure 7: Transverse shunt impedance calculated via Eq. (4). Green curve is $R_{sh,\perp}$ due to Eq. (2) and numerically obtained vertical geometric factor and transverse characteristic impedance. Blue curve is the GdfidL data implemented in to Eq. (4).

SUMMARY

Analytical equations at low frequency for the beam impedances as well as the ratio between $Z(k)_{||,\perp}$ and $R_{sh,||,\perp}$ have been presented. Good agreement is found between the analytical results and 3D GdfidL simulations at low frequencies.

REFERENCES

- [1] R. Shafer, IEEE Trans. Nucl. Sci. **NS-32**, 1933 (1985).
- [2] G.R. Lambertson, “Dynamic Devices-Pickups and Kickers,” in *Physics of Accelerators*, eds. M. Month and M. Dienes, AIP conf Proc. **153**, 1414 (1987).
- [3] D. A. Goldberg and G. R. Lambertson, “Dynamic Devices a Primer on Pickups and Kickers” LBL-31664, Nov. 1991.
- [4] K.-Y. Ng, “Impedances of Stripline Beam-Position Monitors,” Particle Accelerators, 1988, Vol. 23, pp. 93-102.
- [5] J. H. Billen and L. M. Young, Poisson Superfish, LANL.
- [6] R. E. Collin, *Field Theory of Guided Waves* (John Wiley & Sons, New York, 1991).
- [7] W. Bruns, GdfidL, <http://www.gdfidL.de>.